Iterative least-square inversion for amplitude balancing[a]

[a]Published in SEP report, 89, 167-178 (1995)

Arnaud Berlioux and William S. Harlan[1]

ABSTRACT

Variations in source strength and receiver amplitude can introduce a bias in the final AVO analysis of prestack seismic reflection data. In this paper we tackle the problem of the amplitude balancing of the seismic traces from a marine survey. We start with a 2-D energy map from which the global trend has been removed. In order to balance this amplitude map, we first invert for the correction coefficients using an iterative least-square algorithm. The coefficients are calculated for each shot position along the survey line, each receiver position in the recording cable, and each offset. Using these coefficients, we then correct the original amplitude map for amplitude variations in the shot, receiver, and offset directions.

INTRODUCTION

In 1994, Mobil provided SEP with a marine dataset on which we were to perform an amplitude variation with offset (AVO) analysis. However, Berlioux and Lumley (1994) showed that the amplitude of the traces in the survey present anomalies that need to be preprocessed prior to the AVO analysis.

Fluctuations of the source strength and the receiver amplitudes as well as near-surface irregularities can create amplitude anomalies. It is therefore often necessary to balance the amplitude of each trace in the survey.

To do so we determine the source, receiver, and offset amplitude balancing coefficients by using an iterative least-square algorithm. We then apply these scaling factors to the original 2-D amplitude map to cancel the effect of the impulse response of the defective sources and receivers, and to compensate for irregularities of the sea bottom.

[1]**e-mail:** arnaud@sep.Stanford.EDU, harlan@sep.Stanford.EDU

THE PROBLEM OF VARIATIONS OF AMPLITUDE DURING A SURVEY

In a seismic survey, the amplitude recorded at each receiver for each shot depends on the geology of the earth, and on the seismic source and receiver impulse responses. Geophysicists and geologists are interested in the variations of the impulse response of the earth. The impulse responses of the receivers and the source may vary, causing anomalous fluctuations of the amplitude recorded during the experiment. It is therefore necessary to correct for such fluctuations, when observed, in order to restore the earth component, which is the valuable information.

Figure 1 shows an amplitude plot in source and offset coordinates for a 2-D seismic survey provided by Mobil in 1994. For each shot and each offset position (i.e., for each trace of the survey) the value of the amplitude has been calculated by taking the root mean square of the trace amplitudes along the time axis. The global trend (low-frequency component of the earth) of the amplitude surface has been estimated by least-square fitting, and removed from the original surface to leave a globally flat 2-D amplitude map (Berlioux and Lumley, 1994).

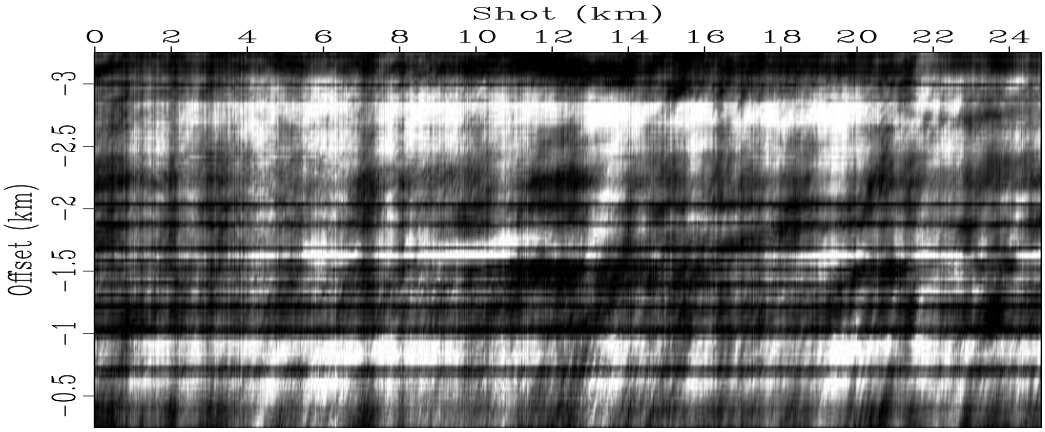

Figure 1: 2-D amplitude plot after removal of the global trend and normalization by the root-mean-square value.

Figure 1 shows the result after normalization by the root-mean-square value of the amplitude. In this figure the horizontal stripes correspond to offsets where the hydrophone had an impulse response that was weaker (darker stripe) or stronger (brighter stripe) than the average response of the other receivers. Likewise, the vertical stripes indicate where the source had an impulse response that varied from the average. Less obvious, though noticeable, are two other categories of stripes dipping to the left. One is quite visible at the bottom of the plot around the offset -0.5 km, dipping at approximately 10 degrees. An example of the second type of stripe, which dips 20 degrees to the left, is visible at the source position 16 km. Based on the amplitude plot in Figure 1, we have built a model of offset-, source-, midpoint-, and receiver-consistent stripes (Figure 2). Comparing both figures we can identify the

first category of dipping stripes as being midpoint-consistent, whereas the less steep stripes are receiver-consistent. The stripes in the receiver directions are broader than the others and therefore not as visible in the source and receiver coordinate system (Figure 3). The stripes in the offset direction follow the descending diagonal in the transformed coordinate system.

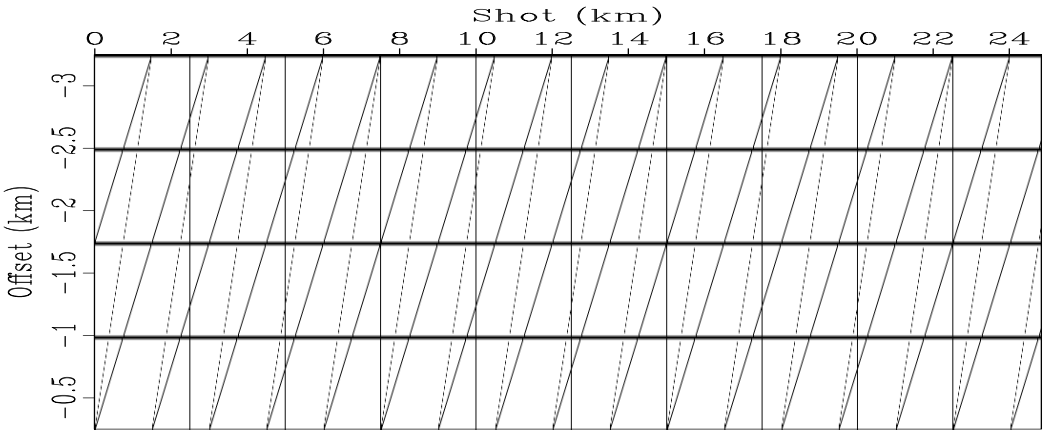

Figure 2: Model of offset-, source-, midpoint-, and receiver-consistent stripes, based on the 2-D amplitude plot in Figure 1. The solid dipping lines correspond to the receiver-consistent stripes, and the dotted lines represent the midpoint-consistent stripes.

Berlioux and Lumley (1994) and Lumley et al. (1995) proposed a method to estimate the source and offset correction coefficients in order to balance the amplitude of each trace in the survey. This method, based on a simple amplitude model, produces good results but does not take into account the receiver-consistent stripes still visible after correction. Because water has a substantially lower velocity than the underlying sediments, the waves travel nearly vertically in the water. The variations of the amplitude caused by the receiver can therefore be associated with near-surface anomalies or irregular sea-bottom topography that affects the receiver recording vertically above it. In the next section, we use a more complex amplitude model, which allows for these variations, and propose an iterative method to estimate the coefficients in order to later correct the amplitude map and balance each trace of the survey.

AN ITERATIVE LEAST-SQUARE INVERSION SCHEME

Our revised amplitude model is

$$a_{s,h}^{total} \;=\; a_s \, a_h \, a_{y=s+h/2} \, a_{r=s+h} \, a_{earth} \tag{1}$$

where a_{earth} is the earth low-frequency component of the amplitude function; and a_s, a_h, a_y, and a_r are the components of the amplitude caused by the source (s), the full offset (h), the midpoint (y), and the receiver (r) variations, respectively.

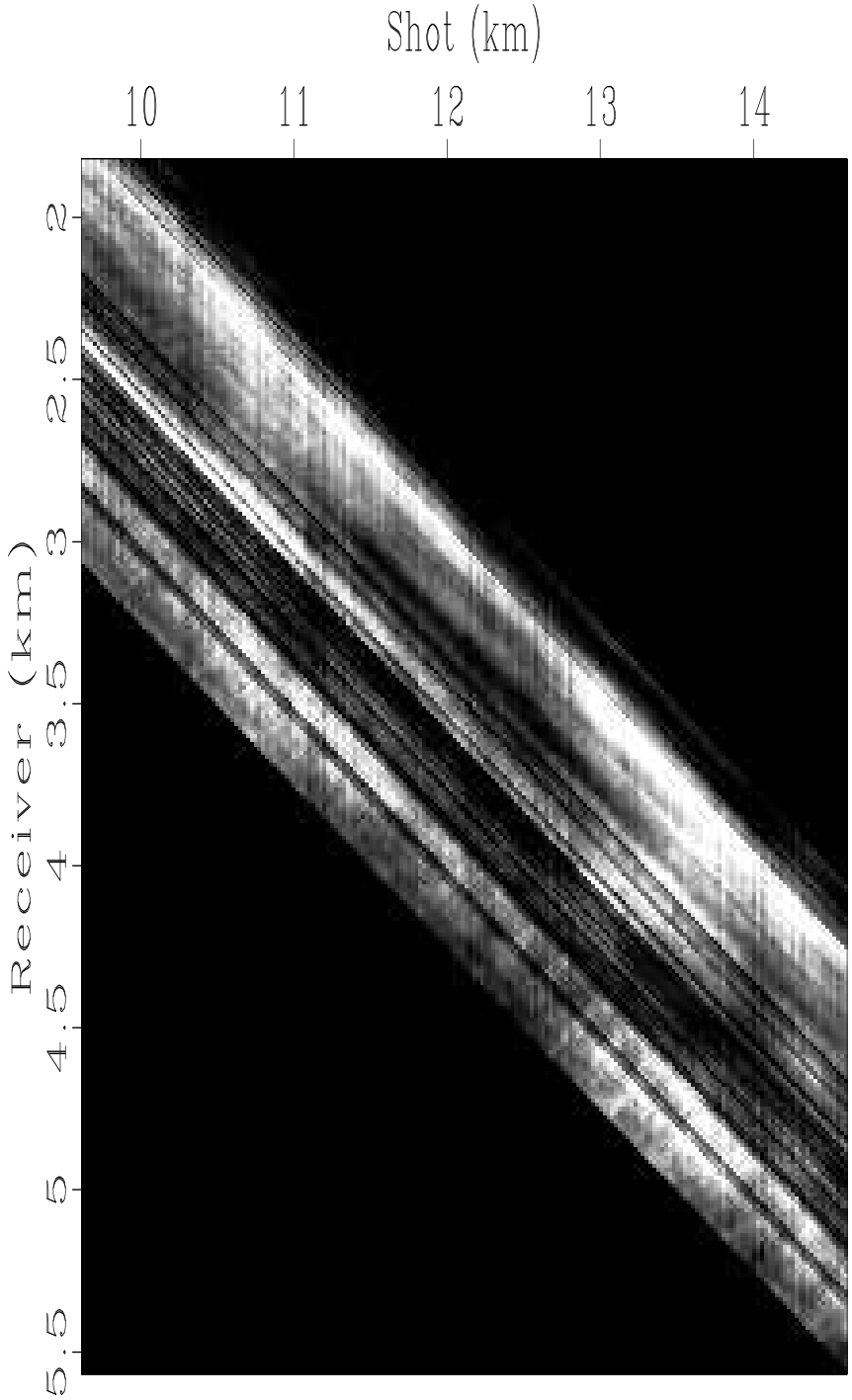

Figure 3: Portion of the amplitude map in Figure 1 displayed in the source and receiver space. The stripes along the descending diagonal follow the offset direction. Midpoint and receiver stripes are less visible in this coordinate system.

We now need to invert for the amplitude correction coefficients in order to remove the stripes in Figure 1. To do so, we use the following quadratic objective function

$$\varphi \;=\; \parallel \; d\;(s,h) \;-\; a_s\, a_h\, a_y\, a_r \;\parallel^2 \tag{2}$$

where we assume that the data d can be modeled as the product of the source, offset, midpoint, and receiver. Normalization allows us to assume $a_{earth} \approx 1$.

To estimate the coefficients a_s, a_h, a_y, and a_r we choose the Gauss-Seidel algorithm which is an iterative least-square inversion scheme [see Stark (1970)]. We also assume that the coefficients for which we are solving the objective function φ are independent. Therefore, we can get an estimation of one type of coefficient (a_s, a_h, a_y, or a_r) while keeping the value of the other fixed.

Under these assumptions, after minizing the objective function with respect to the source coefficients, we derive the following expression, giving the value of the coefficients at iteration k as a function of the other coefficients at the preceding iteration:

$$a_s^{(k)} \;=\; \frac{\sum_h \; d\; a_h^{(k-1)}\; a_y^{(k-1)}\; a_r^{(k-1)}}{\sum_h \; \left[a_h^{(k-1)}\; a_y^{(k-1)}\; a_r^{(k-1)}\right]^2} \tag{3}$$

We obtain a similar expression for the other three coefficients, where each is expressed as a function of the data and all the other coefficients.

Figures 4, 5, 6, and 7 show the result of the inversion when the algorithm has converged, which required 10 iterations. Comparing the source and offset correction coefficient curves (Figures 4 and 5) with those obtained by Berlioux and Lumley (1994), we can see that the global shape of the curves is the same. The curves in Figures 4 through 7 show identical features: high-frequency variations of the coefficient value around a globally constant value.

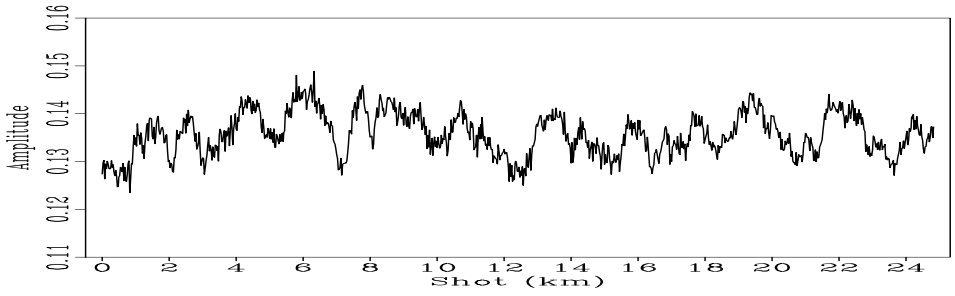

Figure 4: Estimated source coefficients.

The next section shows how we use these estimated correction coefficients to cancel the stripes in the original 2-D amplitude map, and thus balance the traces in the survey.

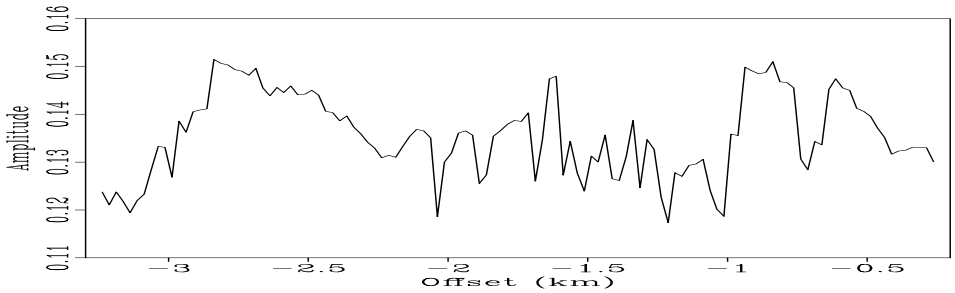

Figure 5: Estimated offset coefficients.

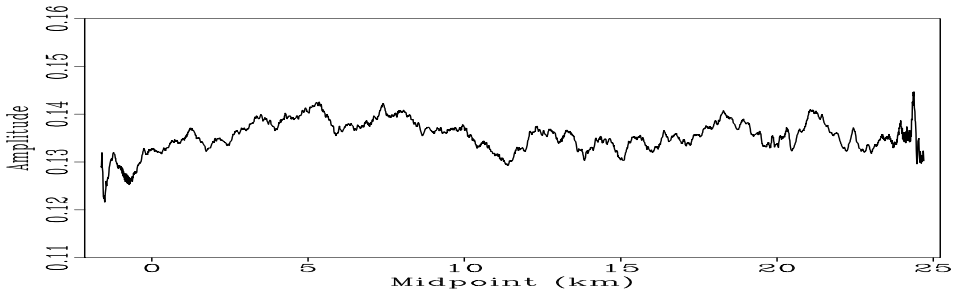

Figure 6: Estimated midpoint coefficients.

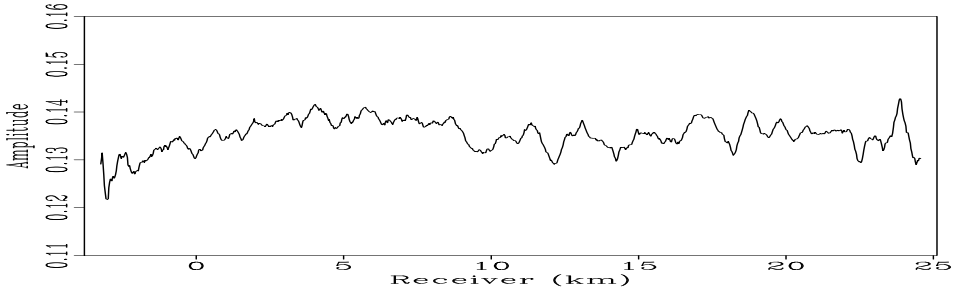

Figure 7: Estimated receiver coefficients.

AMPLITUDE BALANCING

We use the coefficients calculated for the source, offset, and receiver directions to remove the stripes from the plot in Figure 1. Figure 8 shows the 2-D synthetic amplitude map modeled using the source and offset coefficient curves only. The similarity between the stripes in the amplitude plots in Figures 1 and 8 is quite strong.

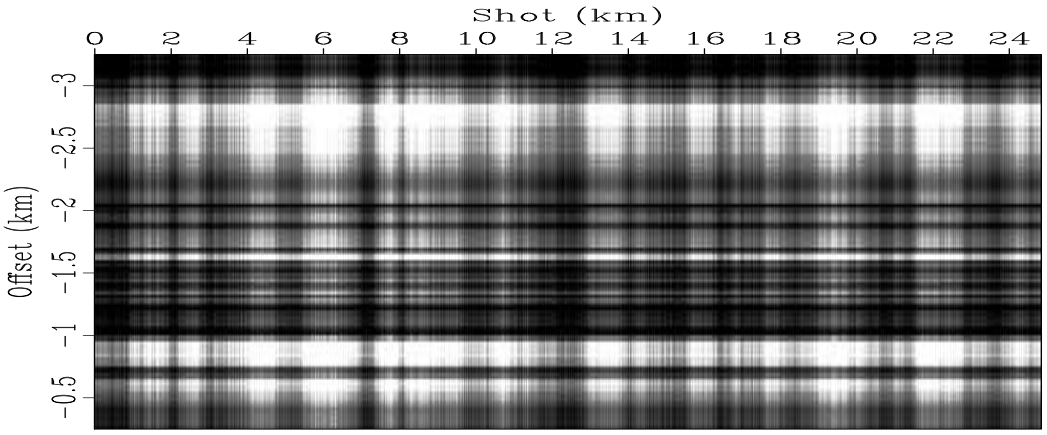

Figure 8: Synthetic 2-D amplitude map modeled using the source and offset coefficients.

We divide the original 2-D amplitude function by the source and offset correction coefficients to obtain the amplitude map in Figure 9. In this plot most of the source- and offset-related anomalous amplitude stripes seem to have disappeared, revealing the grey background (the earth impulse response and noise) and other stripes dipping to the left.

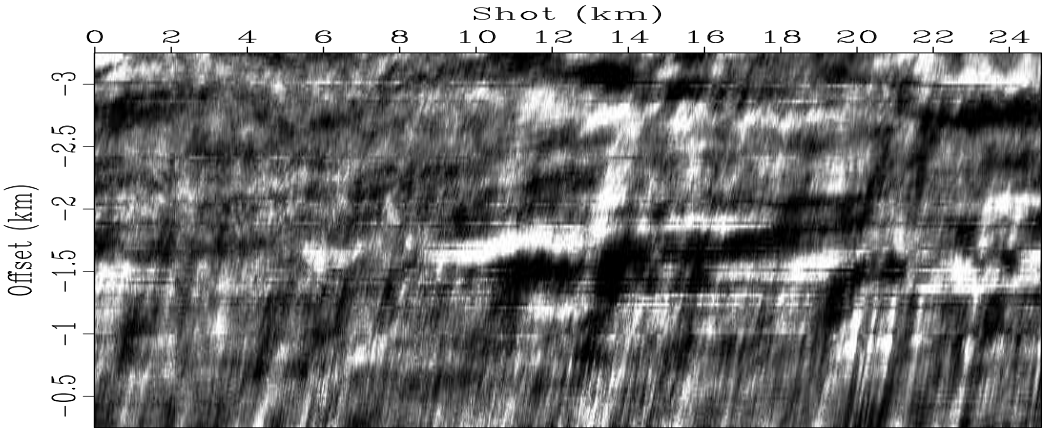

Figure 9: 2-D amplitude map corrected for variations in the source and offset directions using the coefficient curves in Figures 4 and 5.

Comparing Figure 9 and the modeled stripes in Figure 2, we can associate the now more apparent dipping stripes with the receiver- and midpoint-consistent stripes.

In Figure 9, the fine stripes with a steep dip particularly visible at the bottom part of the plot can be regarded as midpoint-consistent, whereas the less steep stripes are receiver-related.

Figure 10 represents a portion of the amplitude map in Figure 9 in the source and receiver coordinate system. The plot shows a bright spot smeared along the offset direction (the descending diagonal). Two very broad darker stripes orthogonal to the receiver axis are visible around the receiver positions at 9.5 km and 12 km. In this coordinate system we can identify these two broad stripes as receiver-consistent. This observation is confirmed by Figure 7, in which the receiver correction coefficient curve shows two local minima at the corresponding receiver location. The same stripes are also noticeable in the center of the plot in Figure 9, though less obvious. They are also clearly visible in Figure 11, which is a synthetic amplitude map modeled from the receiver coefficients only.

Figure 12 shows the amplitude map corrected for variations in the source, offset, and receiver directions. It is the result of the division of the plot in Figure 9 by the estimated receiver coefficients in Figure 7. Figure 13 represents the portion of the corrected amplitude map in Figure 12 in the source and receiver coordinate system. After the correction has been applied, the broad horizontal stripes around the receiver positions at 9.5 km and 12 km have disappeared.

Although midpoint-consistent factors are not used to correct the data amplitudes, we invert for the factors simultaneously to separate the different components more fully. The resulting amplitude map, corrected for anomalous variations in the source, offset, and receiver directions, shows the contribution of the earth and midpoint components to the amplitude of the recorded traces. Some variations may still be present, but not dominant.

CONCLUSIONS

Using a more complex amplitude model than that described by Berlioux and Lumley (1994), we have estimated the correction coefficients to balance the trace amplitudes of the Mobil AVO dataset. For this model, we have assumed that the coefficients we are inverting for are independent. We have corrected the original 2-D amplitude map with the source, offset, and receiver coefficients determined by an iterative least-square inversion scheme. This new method gives a more accurate result, taking into account variations of the amplitude caused by the receivers. The stripes in the source, offset, and receiver directions have been successfully removed to reveal the geological grey background of the amplitude plot. We believe the same algorithm can be used for other data sets that present a similar amplitude balancing problem.

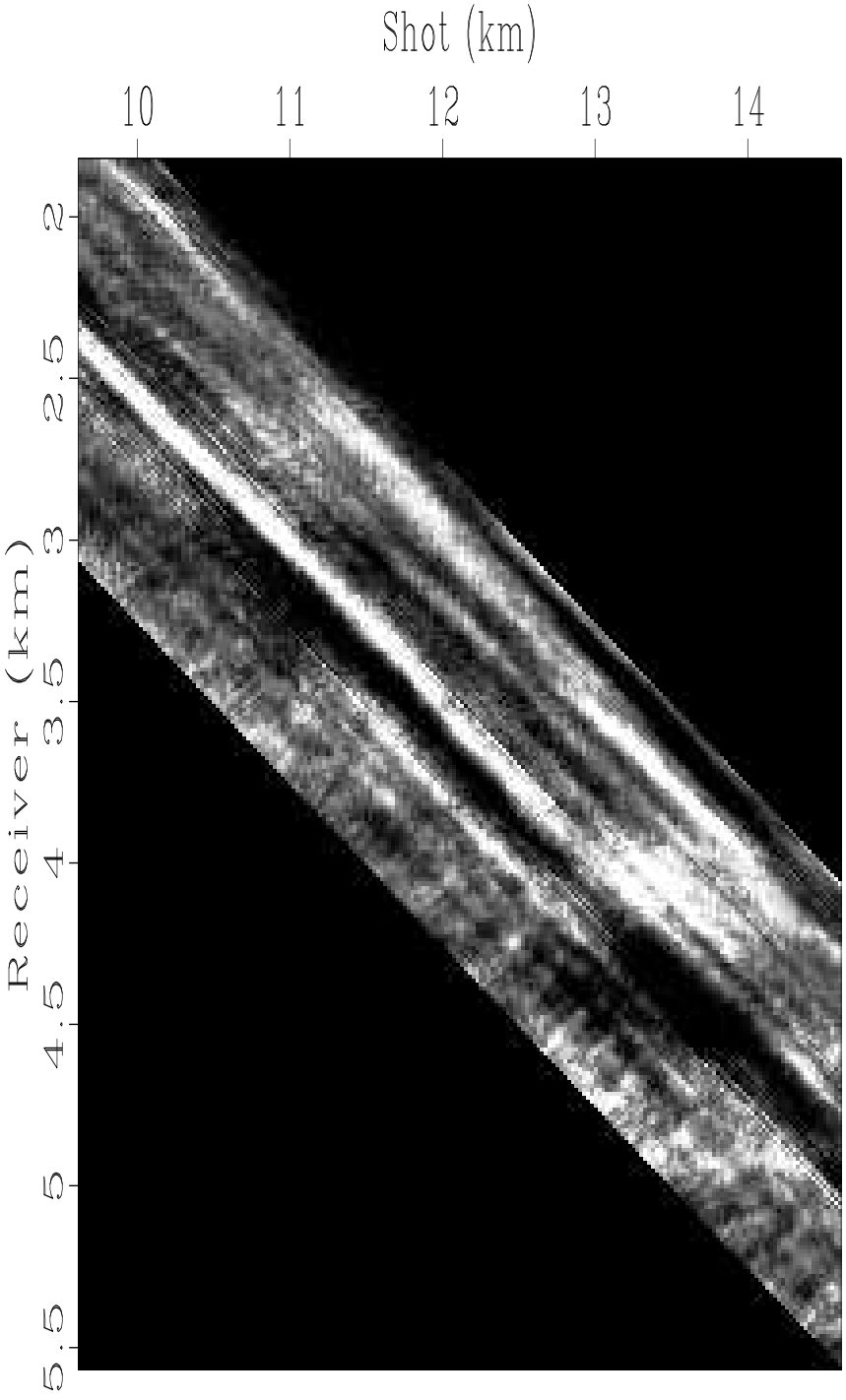

Figure 10: Portion of the amplitude map in Figure 9 displayed in the source and receiver space.

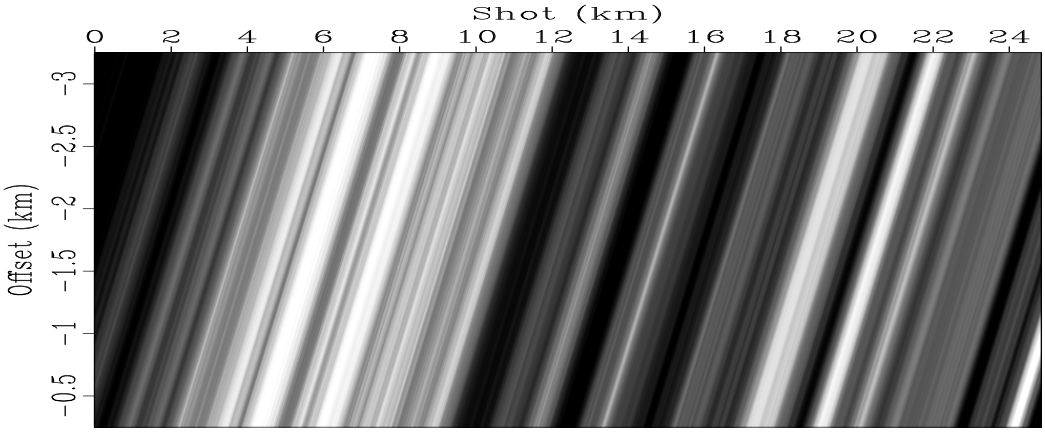

Figure 11: Synthetic 2-D amplitude map modeled using the receiver coefficients.

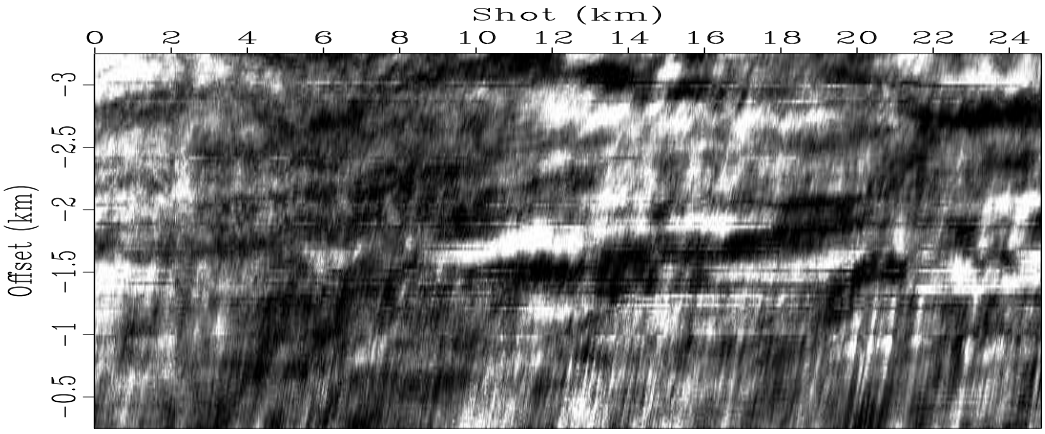

Figure 12: 2-D amplitude map corrected for variations in the source, offset, and receiver directions using the coefficient curves in Figures 4, 5, and 7.

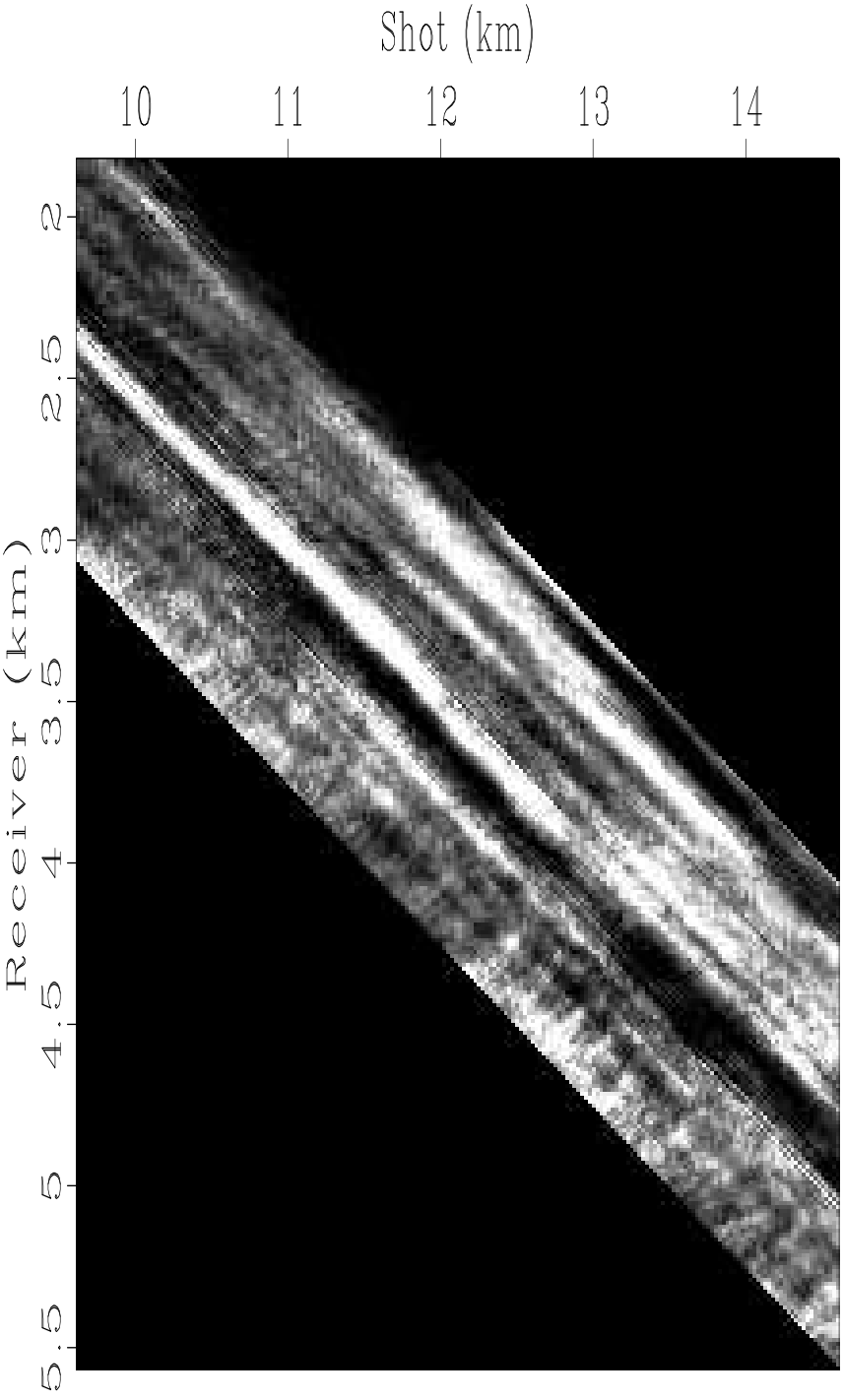

Figure 13: Portion of the corrected amplitude map in Figure 12 displayed in the source and receiver space.

REFERENCES

Berlioux, A., and D. Lumley, 1994, Amplitude balancing for AVO analysis, *in* SEP-80: Stanford Exploration Project, 349–360.

Lumley, D. E., D. Nichols, C. Ecker, T. Rekdal, and A. Berlioux, 1995, Amplitude-preserved processing and analysis of the Mobil AVO data set, *in* SEP-84: Stanford Exploration Project, 125–152.

Stark, P. A., 1970, Introduction to Numerical Methods: MacMillan Publishing Co., Inc.